Lujan Martinez, JM.; Guardiola García, C.; Plá Moreno, B.; Cabrera López, P. (2014). Considerations on the low-pressure exhaust gas recirculation system control in turbocharged diesel engines. International Journal of Engine Research. 15(2):250-260. doi:10.1177/1468087413485209.

Considerations on the low pressure EGR system control in turbocharged diesel engines

José Manuel Luján, Carlos Guardiola, Benjamím Pla, Pedro Cabrera

CMT Motores Térmicos, Universidad Politécnica de Valencia, Camino de Vera s/n, E-46022 Valencia, Spain

Abstract

Although high pressure exhaust gas recirculation has been commonly used in turbocharged diesel engines for controlling the NOx formation, recent advances in after-treatment and material technology make possible using a low pressure architecture, which recirculates the exhaust gas upstream the compressor. This brief paper presents a basic study of control aspect related to the low pressure architecture, emphasising the similarities and differences with the high pressure system. Data coming from experimental tests with both configurations, and from a one-dimensional wave action model simulations, are combined for the analysis of the input-output paring, linearity and the transient performance of both systems.

Keywords: Diesel engine, engine control, exhaust gas recirculation, turbocharging, model predictive control.

Email addresses: jlujan@mot.upv.es (José Manuel Luján), carguaga@mot.upv.es (Carlos Guardiola), benplamo@mot.upv.es (Benjamím Pla), pedcablo@mot.upv.es (Pedro Cabrera)

Nomenclature

BGF	burnt gas fraction
m_a	air mass flow
p_2	boost pressure
X	actuator position
λ	relative air-to-fuel ratio
BMEP	brake mean effective pressure
BPV	back pressure valve
DPF	diesel particulate filter
DOC	diesel oxidation catalyst
ECU	electronic control unit
EGR	exhaust gas recirculation
HP	high pressure
LP	low pressure
LTC	low temperature combustion
NOx	nitrogen oxides (at exhaust)
O2	(intake manifold) oxygen
VGT	variable geometry turbine

1. Introduction

Exhaust gas recirculation (EGR) has become a widespread technique for controlling nitrogen oxides (NOx) formation and emission in current automotive turbocharged diesel engines [1, 2]. Although low pressure (LP) EGR is not a new technical solution and has been known for long [3], it has been traditionally discarded because compressor wheel damaging and soiling and acid corrosion problems in the intercooler [4]. Hence, high pressure (HP) EGR system is currently the standard solution. However, new engine technologies, like particulate filters for exhaust gas after-treatment [5], the development of high resistance intercoolers [6] and the generalization of low sulfur content fuels, could allow using low pressure EGR systems.

HP-EGR system control has been a major topic of research because it is strongly coupled with the turbocharging system [7, 8, 9, 10, 11, 12, 13, 14, 15]. On the contrary, LP-EGR has not been deployed in series engines until recently and limited research has been conducted in this topic, and particularly about LP-EGR control [16]. This paper compares the two systems and analyses the advantages and disadvantages of the LP-EGR system from the control point of view. For the present study, simulation results from a one dimensional engine code and experimental results are combined.

2. Engine model and experimental facility

The engine used for the study is a 2-litre 4-cylinder turbocharged diesel engine whose main characteristics are provided in Table 1. The series engine has a variable geometry turbine (VGT) for boost pressure control and a HP-EGR with an electrically piloted valve for the EGR rate control.

For the present work, an auxiliary LP-EGR system and a water cooled intercooler were installed as sketched in Figure 1. A back pressure valve (BPV) was used for raising the pressure drop in the exhaust system, thus increasing the EGR rate in the cases when EGR valve was fully

Table 1: Engine main characteristics

Displacement	1998 cm^3
Bore x Stroke	85 x 88 mm
Valves	4 / cylinder
Compession ratio	18:1
Turbocharger	Garret VNT GT 1749V
After-treatment	Oxi-catalyst + DPF
Certification	EURO-IV compliant
Max. power / speed	100 kW / 4000 rpm
Max. torque / speed	320 Nm / 1750 rpm

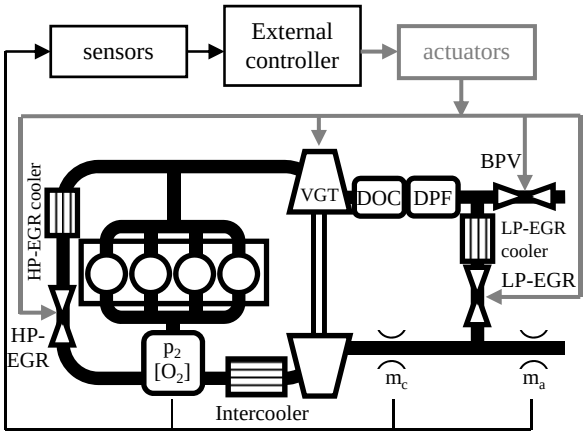

Figure 1: Lay-out of the experimental facility.

open but pressure difference between the exhaust and intake was not sufficient for attaining the desired EGR rate.

An external control system was used for controlling EGR valves and VGT, while the engine was instrumented with an intake manifold pressure sensor, two hot wire anemometers (upstream and downstream the LP-EGR junction) and a broadband lambda sensor for intake manifold gas composition determination. All these sensors are similar in quality and characteristics to the sensors used for production engines. This was preferred to using research grade sensors in order to ensure the applicability of the results.

EGR valves and BPV were electrically actuated, while an electropneumatic VGT was used [17]. A cascade control was implemented with a low-level feedback based on valve position; hence air-path control system just sets the reference position of the valves (X_{VGT}, X_{VGT} or X_{BPV}). Since the deviation between the reference position and the actual position was not significant for the studied points, in the hereinafter only the reference position will be shown in the paper plots.

Additionally to the experimental facility, a wave action model (OpenWAM) [18] was used for simulating the engine operation. OpenWAM is a freeware simulation tool developed at CMT-Motores Térmicos based on a one-dimensional code with specific sub-models for turbocharger

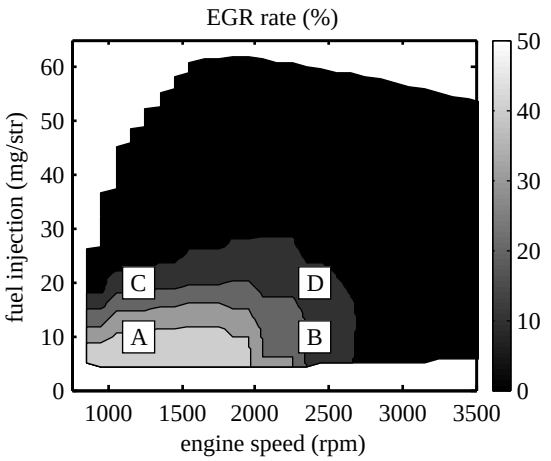

Figure 2: Engine operation map indicating EGR level and operation maps listed .

[19] and combustion process modelling [20]. Finally OpenWAM is linked with Matlab for control system simulation and evaluation [21]. Complete model fitting process is described in [22, 20], while some application showing the performance of the model may be found in [17, 23].

For the present research, engine model was validated using specific engine tests. Accuracy metrics of the model fit to this engine operating when operating with the HP-EGR circuit are reported in [24]. Because of the physical approach used in the fluid dynamics model, it is able to properly describe the instantaneous evolution (including in-cycle pulsation) of gas temperature, speed, composition and pressure at any point of the engine air-path. However, due to the simplification inherent to the one-dimensional description of the system, three-dimensional effects may not be described by this kind of models [25].

Regarding the engine conditions analysed, four different points (Table 2) were selected from the engine map representing different conditions of engine speed and load within the EGR zone, as depicted in Figure 2.

Table 2: Operating conditions as a function of engine speed and injected fuel quantity.

	1200 rpm	2400 rpm
10 mg/str (3 bar BMEP)	A	B
20 mg/str (6 bar BMEP)	C	D

3. Sensor selection

The problem of the air management system control starts with the sensor selection. The most common choice in current turbocharged engines is to use the air mass flow and the intake pressure as control variables. This selection is justified by the availability of mass flow and

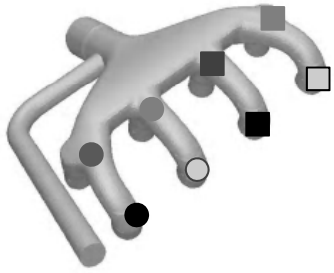

Figure 3: Location of the intake manifold probes for the experiment. Symbols are correspondent to the results shown in Figure 4.

pressure sensors with high accuracy and reliability at affordable costs. However, some studies suggest the use of lambda sensors as an alternative to improve fuel consumption while controlling emissions [26, 27, 28].

According to [29], the use of parameters such as the EGR fraction or the oxygen-to-fuel ratio instead of the traditional air mass flow and intake pressure as feedback variables involves important advantages due to their more straight-forward effect on engine performance and emissions.

Nevertheless, the introduction of these oxygen-related variables also involves some challenges, and the most important one is probably the availability of reliable, accurate and feasible sensors. Despite the EGR fraction can be estimated using observers [12], heated wide range lambda sensors may be used for measuring the oxygen concentration in the intake manifold [30]. Since those sensors are sensitive to pressure, the measured signal has to be corrected to avoid the effects of the intake manifold pressure.

In addition the intake concentration measurement may be also affected by the sensor location, as reported in [24]. When the air and the EGR gas are not properly mixed in the intake manifold, the lambda sensor can provide a measurement which is not representative of the mean oxygen concentration in the intake manifold. While the problem of the pressure correction has been properly addressed, for example in [30], the authors have not find studies considering the problem of the sensor positioning.

To deal with this last aspect, an experiment consisting on using eight alternative probes located at the eight engine intake runners was performed [24], as depicted in Figure 3. Each of the probes was used for feeding a NDIR gas analyser which determined the intake CO_2 concentration, and from this the intake burnt gas fraction (BGF) at the eight intake ports.

Figure 4 shows, for a steady test run at 1200 rpm and 10 mg/str (conditions A), the probability distribution of the CO_2 concentration in the intake manifold gas when extracting from the different probes installed at the intake manifold locations shown in Figure 3. Mean value of the distribution is related with the mean concentration at the probe location, while distribution dispersion is attributed to intra-cycle variations and the existence of unavoidable measurement and operation errors. Left plot in Figure 4 shows the results for the engine operating with the HP-EGR loop, while right plot reports the results for the LP-EGR. In the case of the HP-EGR system, Differences in the CO_2 concentration obtained from the different probes are significantly high, and it may be concluded that a dispersion exists in the charge concentration in each one of

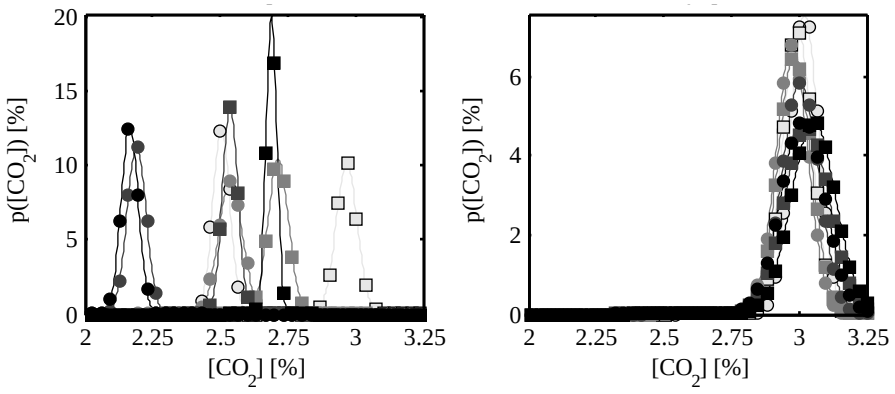

Figure 4: Probability distribution of the CO_2 concentration in 8 different probes at the intake manifold for the HP-EGR system (left) and the LP-EGR system (right) at A conditions (1200 rpm and 10 mg/str). Symbols correspond to those marked in the probes in Figure 3.

the cylinders. On the other hand, when the engine was operated with the LP-EGR architecture, all probes provide a similar mean measurement, as shown in right plot in Figure 4.

This lack of homogeneity in the HP-EGR configuration can have important effects on the engine operation. On one hand, the non homogeneity can imply that each individual cylinder has different gas composition, which could impact the engine out emissions, and even the stability of the combustion if low temperature combustion (LTC) methods are used [31, 32]. On the other hand, this fact implies a great difficulty for the implantation of intake gas composition sensors (as broadband lambda sensors): the measurement provided by the sensor can be not representative of the mean BGF.

Correcting the deviation of the sensor is not straightforward as it varies in a non-linear way. Furthermore, the homogeneity is strongly dependent on the operating conditions, since the wave pattern established in the manifold is critically affected by the engine speed, and also by the recirculated burnt gas fraction.

In opposition, LP-EGR architecture is not affected by these effects: the long path used along the intake system (including the pass through the compressor) ensures an homogeneous composition of the gas mix. Hence, all cylinders have the same admitted gas composition, and its value can be easily determined through a sensor in the intake manifold. Therefore, the LP-EGR architecture involve some advantages when using a lambda sensor as an alternative to control the EGR-VGT systems.

4. Static gain analysis

In the classical HP-EGR architecture, the coordination of the VGT and EGR actions leading an optimal engine performance is a challenging task due to the strong coupling between the two systems [8, 29]. To address this aspect, after fitting the model to experimental data, a set of simulations of steady conditions with constant injected fuel mass quantity and engine speed, and different EGR valve and VGT positions were performed. The simulations were also replied in the LP-EGR configuration.

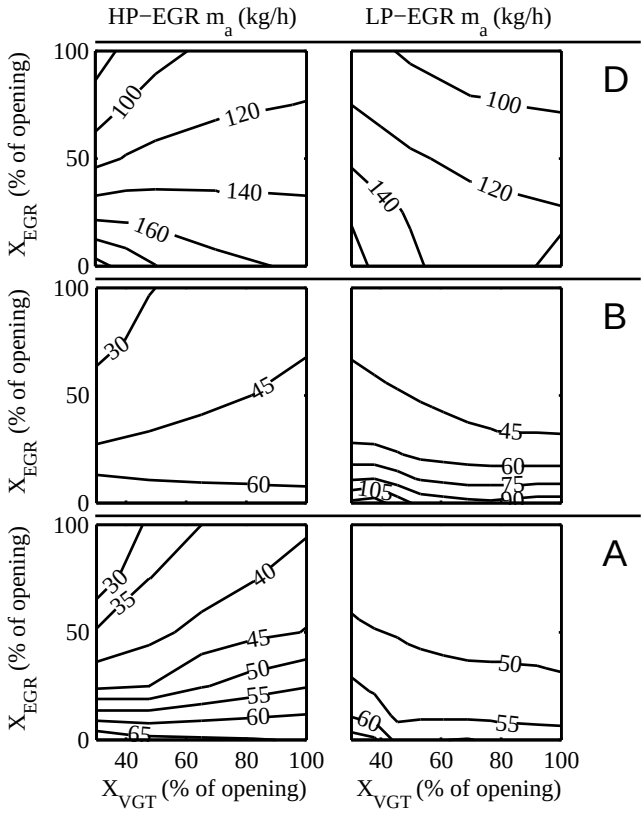

Figure 5: Maps of m_a when varying EGR and VGT positions for the HP-EGR system (left) and the LP-EGR system (right). Obtained from the engine model at 2400 rpm and 20 mg/str (D, upper plots), 2400 rpm and 10 mg/str (B, medium plots) and 1200 rpm and 10 mg/str (A, lower plots) conditions.

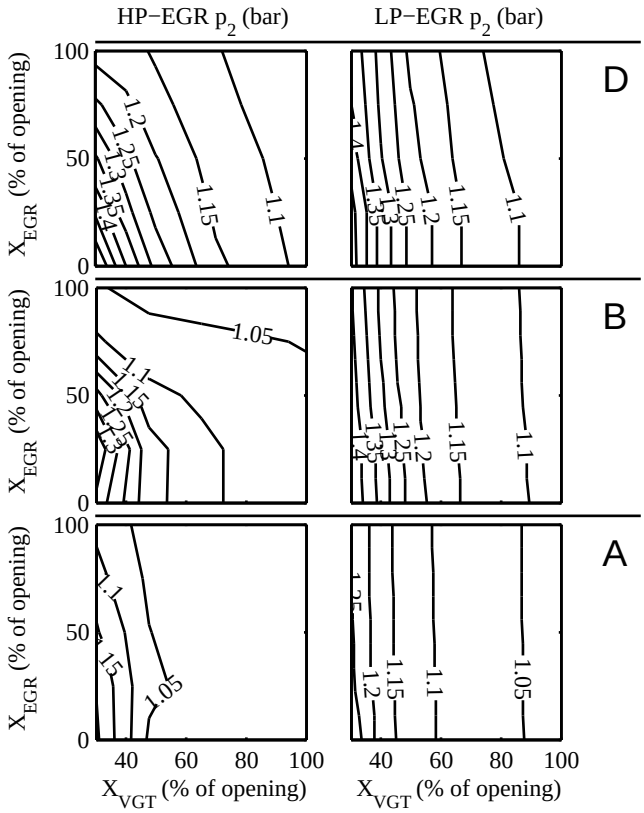

Figure 6: Maps of p_2 when varying EGR and VGT positions for the HP-EGR system (left) and the LP-EGR system (right). Obtained from the engine model at 2400 rpm and 20 mg/str (D, upper plots), 2400 rpm and 10 mg/str (B, medium plots) and 1200 rpm and 10 mg/str (A, lower plots) conditions.

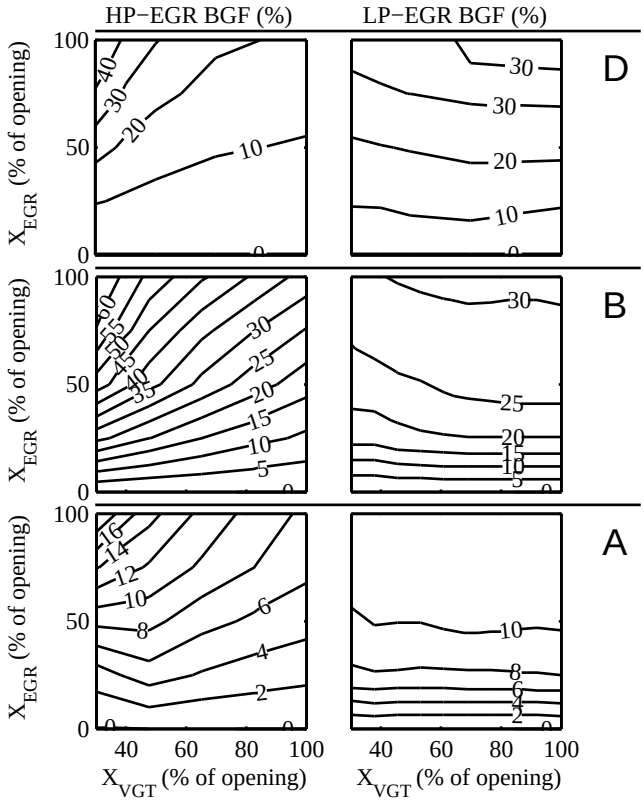

Figure 7: Maps of *BGF* when varying EGR and VGT positions for the HP-EGR system (left) and the LP-EGR system (right). Obtained from the engine model at 2400 rpm and 20 mg/str (D, upper plots), 2400 rpm and 10 mg/str (B, medium plots) and 1200 rpm and 10 mg/str (A, lower plots) conditions.

Maps in Figures 5 to 7 summarise the results of these simulations, where the steady interactions between the VGT and EGR systems and their effects on air mass flow (m_a), intake pressure (p_2) and intake burnt gas fraction (BGF) are shown. The upper row of each figure contains the results obtained at the engine conditions with the highest power demands (D), the medium row shows the air-loop behaviour at B conditions, while the lower row presents the effects of EGR valve and VGT opening at point A, with the lowest power requirements. On the other hand, the left column contains the results obtained with the HP-EGR loop, while results for he LP-EGR layout appear in the right column.

Figure 5 shows the static maps of air mass flow as a function of VGT and EGR positions for the two studied EGR architectures. For the three conditions analysed, the air mass flow through the engine increases as the VGT closes if the EGR valve remains closed. However, as the HP-EGR valve opens, the increase in the air mass flow as the VGT closes is progressively reduced until an EGR opening in which the VGT does not affect the air mass flow is reached. This EGR opening in which there is not appreciable effect of the VGT position on air mass flow depends on the engine operating conditions. According to the results shown in Figure 5, the higher the power demand, the higher the EGR opening in which the gain between the VGT position and air mass flow is zero, and therefore the wider the zone in which closer VGT positions involve higher air mass flows. If the EGR valve opening increases even more, closing the VGT gives rise to lower air mass flows. In fact, closing the VGT vanes leads to an increase in the exhaust pressure. If the HP-EGR valve is closed, the whole exhaust mass flow will go through the turbine, accelerating the turbocharger and increasing the mass flow through the compressor. Nevertheless, as the EGR valve gets open the increase in exhaust pressure also leads to an increase in the recirculated flow, then reducing the air mass flow. Both effects, which are opposite, provide a gain inversion in the relation between air mass flow and VGT position. The operating conditions at which this gain inversion appears depend on engine parameters such as the engine speed and fuelling rate.

Figure 6 shows the static maps of intake pressure as a function of VGT and EGR positions for both EGR systems. Since the exhaust gas recirculation does not reduce the energy availability at the turbine inlet when LP-EGR is employed, the intake pressures achieved when the EGR valve is open reach higher values with LP-EGR than with HP-EGR loop. In fact, from the orientation of the lines of constant intake pressure it can be stated that the intake pressure is almost independent of the LP-EGR valve opening. This aspect and others related to the signal pairing will be addressed in section 5.

Finally, in Figure 7 the static maps of intake burnt gas fraction as a function of VGT and EGR positions are shown. In this case, it can be observed how the burnt gas fraction of the intake gases is almost independent of the VGT position when the LP-EGR architecture is employed. On the contrary, the VGT position impact on the exhaust gas recirculation increases as the HP-EGR valve gets open. In addition, Figure 7 shows that the LP-EGR system does not allow to achieve EGR rates as high as those obtained with the HP-EGR architecture, this fact is specially important at low speed and load (engine conditions A and B) due to the low air mass flow and then the low pressure difference between DPF outlet and compressor inlet. At those conditions, a BPV placed downstream the EGR extraction or a throttling valve before the EGR discharge is required in order to increase the pressure difference between exhaust and intake lines, thus allowing higher EGR rates.

Results shown in Figures 5 to 7 suggest that the LP-EGR architecture is essentially decoupled if boost pressure and BGF (or oxygen concentration) are considered. This can be considered a clear advantage with regard to the traditional approach, where air mass flow and boost pressure are used as controlled variables. Note that significant differences in the m_a, p_2 and BGF

responses appear depending on engine speed and load and controller parameters must be scheduled in order to be adapted to the engine operating conditions.

Results shown for the tested engine confirm that the behaviour of the EGR system and the gain in the different variables is significantly dependent of the operating conditions. This is rooted in the complex coupling between the engine, the compressor and the turbine. As a consequence, the extrapolation of the reported results for different diesel engines will be conditioned by the specific engine selected and by the effective actuator range and operative conditions. In this sense, it could happen that some of the reported effects for the HP-EGR configuration do not appear in a given diesel engine. However, sign inversions in the HP-EGR configuration are more likely to occur if the engine operates with high EGR rate, which implies a wide EGR valve that may be fully closed during transients. This situation is usual in downsized light duty engines, and can also occur on heavy duty engines operating with high EGR rate.

5. Signal pairing

On the basis of the static gain maps shown in Figures 5 to 7, and using the method proposed by Bristol [33], it is possible to study the convenience of a given input-output pairing. The method is based on studying the coefficients μ_{ij} obtained through the input-output gain matrix Φ, where

$$\mu_{ij} = \Phi_{ij}\left(\Phi^{-1}\right)_{ji} \tag{1}$$

μ_{ij} determines the coupling between input i and output j. $\mu_{ij} = 0$ implies that the given input does not influence the output, while $\mu_{ij} > 0$ marks the relative influence of the input on the output; $\mu_{ij} < 0$ is associated with instabilities in the control. Due to the construction of the coefficients $\sum_j \mu_{ij} = 1$, then, perfect decoupled system occurs with a given $\mu_{ij} = 1$ while the rest of coefficients for the same output are equal to 0. In the case of a 2×2 system, it is evident that $\mu_{11} = \mu_{22}$ and $\mu_{12} = \mu_{21}$.

For the studied system, three different sets of outputs can be selected: $\{m_a, p_2\}$, $\{BGF, p_2\}$ and $\{m_a, BGF\}$. For each one of the sets and each EGR architecture, maps representing the value of μ_{ij} at the studied operating conditions A, B and D in the whole range of regulation of the VGT and EGR valve can be built. The variation of these coefficients can be used for inferring the effect of the EGR and VGT positions on the system controllability.

Figure 8 shows the μ_{ij} maps for the $\{m_a, p_2\}$ set, in HP- and LP-EGR configurations. The maps obtained for the HP-EGR system confirm the convenience of the usual pairing (m_a-EGR and p_2-VGT). Values near 1 show the higher influence of the EGR valve position on air mass flow than on intake pressure, and accordingly, the higher effect of the VGT on intake pressure than on air mass flow. It can be noticed how as the VGT opens, the effect of the EGR valve on air mass flow is progressively reduced, specially at B conditions. Also, Figure 8 shows that in the case of the VGT very closed at D conditions, the risk of instabilities exists if both signals are controlled simultaneously. In that zone $\mu_{HPEGR,m_a} > 1$, so $\mu_{HPEGR,p_2} < 0$. In the case of the LP-EGR system, μ_{LPEGR,m_a} and μ_{VGT,p_2} are in a narrow range arround 1, and therefore an almost perfect decoupling between EGR and VGT is expected.

In case that $\{BGF, p_2\}$ is selected as output pair, the maps of Figure 9 are obtained. As in the previous case, as far as the HP-EGR architecture is concerned the EGR and VGT systems are strongly coupled, although instabilities do not occur in this case. Note that the coupling of the system increases when the VGT is large open, since at these situations the sensitivity of

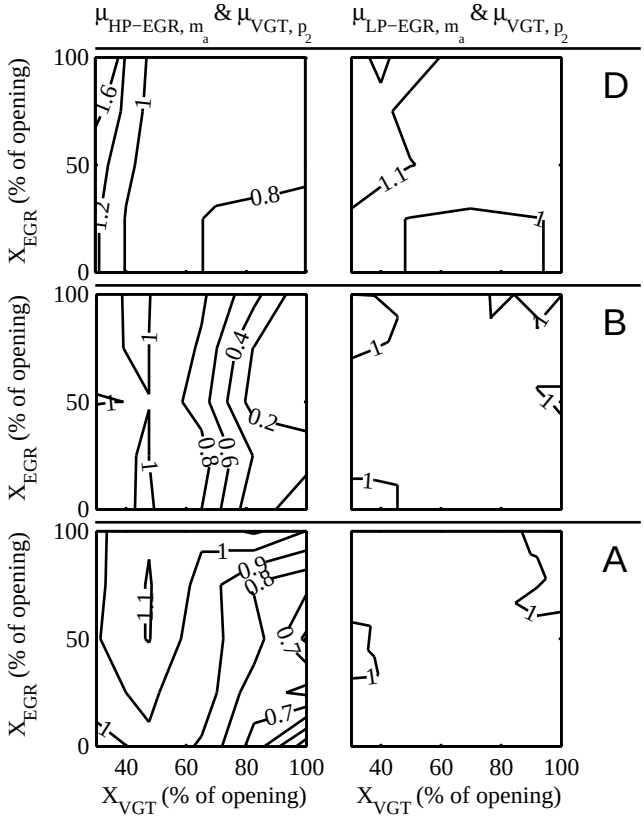

Figure 8: Maps of μ values considering $\{m_a, p_2\}$ set for the HP-EGR system (left) and the LP-EGR system (right). Obtained from the engine model at 2400 rpm and 20 mg/str (D, upper plots), 2400 rpm and 10 mg/str (B, medium plots) and 1200 rpm and 10 mg/str (A, lower plots) conditions.

the system to the EGR valve position is lower. Although it is possible to control the system, multivariable control techniques will be necessary due to the important crossed influence. The suggested pairing for this system is BGF-EGR and p_2-VGT since the effect of the EGR opening on BGF is larger than its effect on p_2, and the opposite for the VGT. On the other hand, the LP-EGR system presents an almost decoupled situation, where VGT can be used for controlling p_2 and EGR for BGF. In fact, it can be stated, that for the LP-EGR loop architecture, the choice of p_2 and BGF as feedback variables allows a better decoupling than the traditional p_2-$m-a$, as can be checked in the slopes of iso-p_2 and iso-BGF lines appearing in Figures 6 and 7 respectively.

Finally, maps for the $\{m_a, BGF\}$ set (not shown) reveal instabilities for both the LP-EGR and HP-EGR cases. This is due to the fact that the EGR position has an important direct influence on both quantities, which are importantly correlated. Hence these two variables must be rejected as control pairs.

Note that, as pointed in the precedent section, results will be dependent of the selected engines, the considered operating points and the actuator range.

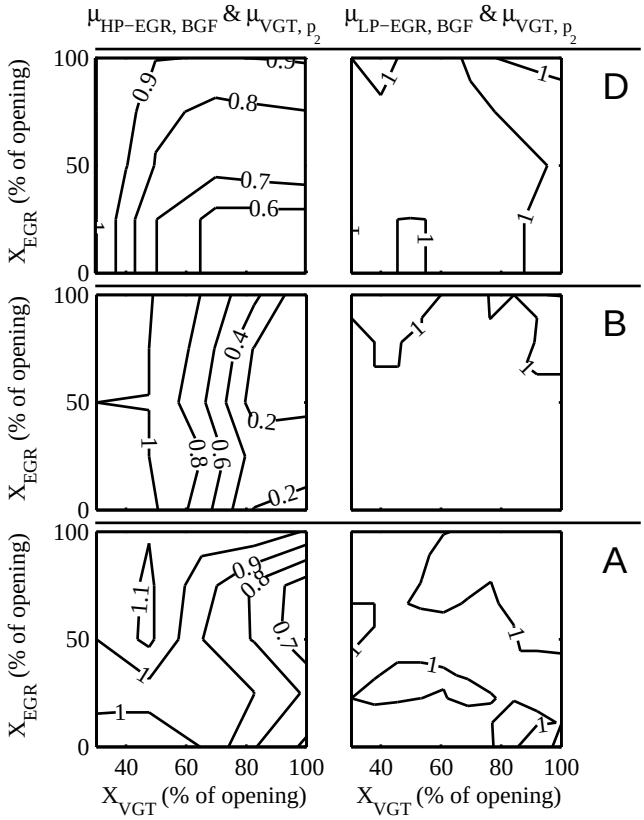

Figure 9: Maps of μ values considering $\{BGF, p_2\}$ set for the HP-EGR system (left) and the LP-EGR system (right). Obtained from the engine model at 2400 rpm and 20 mg/str (D, upper plots), 2400 rpm and 10 mg/str (B, medium plots) and 1200 rpm and 10 mg/str (A, lower plots) conditions.

6. Dynamic analysis

For the analysis of the dynamic response of the system, both simulation and experimental techniques were used. In an initial stage, transient simulations in which step openings were applied to the EGR and VGT were done. Additionally the effect of the BPV was checked for the LP-EGR system. Results on the evolution of the main variables during the simulated transients are shown in Figure 10.

Results for a step in the VGT position appear in left-hand plots. Results are presented for the HP-EGR system (grey) and the LP-EGR system (black) and considering two different operating conditions: closed EGR valve (dotted), and partially open EGR valve (full). Two remarkable effects can be noticed in line with the conclusions of the steady analysis: in LP-EGR configuration VGT do not significantly influences the BGF, and the sign of the variation on m_a on the HP-EGR system when a step in the VGT is applied depends on the EGR position. Both issues confirm that the LP-EGR system is more easily decoupled than the HP-EGR system. Concerning the dynamics of the response in m_a and p_2, no significant differences are noticed between both architectures.

When considering the response to variations in the EGR position (central plots) a significant drawback of the LP-EGR system can be highlighted: there is a huge delay (up to 0.3s) between the EGR step occurrence and the variation of the BGF in the intake manifold. This delay is attributed to long line between the EGR junction and the intake manifold (dotted line represents the BGF just downstream the air-EGR mixing point, showing a similar time response to the HP-EGR system). This delay can compromise the performance of the engine during load steps and specially smoke emissions. As an illustrative example, Figure 11 shows an experiment were a load step was applied, both for LP- and HP-EGR configurations. Due to the control system configuration in the engine ECU, the air mass flow was closed loop controlled but the same VGT position was used, which results of different initial settings for the HP- and LP-EGR tests. During the test, LP-EGR system exhibits an initial faster response in air mass flow, because turbocharger initial speed is higher (alike HP-EGR, LP-EGR does not divert energy from the turbine). However, since the gas in the intake manifold still presents a significant BGF, air-to-fuel relative ratio (λ) drops significantly below 1, what would probably cause a significant smoke spike. In order to avoid that, it would be necessary to completely redefine the fuel limiter calibration for the LP-EGR system, which would impact the engine load response.

Back to Figure 10, another significant difference is that the LP-EGR system avoids the non-minimum phase response that can appear in the HP configuration on the boost pressure (which results from the opposed effects of the fast pressure equalisation in the manifolds and the slow turbocharger dynamics). Finally, LP-EGR system allows the control of the EGR rate through the BPV. The effect of this valve (shown on right-hand plots in Figure 10) is similar to that of the EGR valve. However, it impacts the engine efficiency since it increases the backpressure at the exhaust manifold, and thus it is only foreseen for increasing the EGR rate once EGR valve becomes saturated.

A second study was done experimentally by imposing a pseudo-random binary sequence in both EGR and VGT. The results of such tests for the HP- and LP-EGR systems are shown in Figure 12. Important differences in the gain of the system are noticed depending on the considered EGR architecture. The higher pressure difference in the EGR duct with the HP-EGR architecture leads to a higher influence of the EGR valve opening in the intake O_2 concentration and air mass flow. In addition, since the EGR valve opening hardly affects intake pressure in the LP-EGR configuration, the effect of the EGR opening on intake pressure is also higher for the

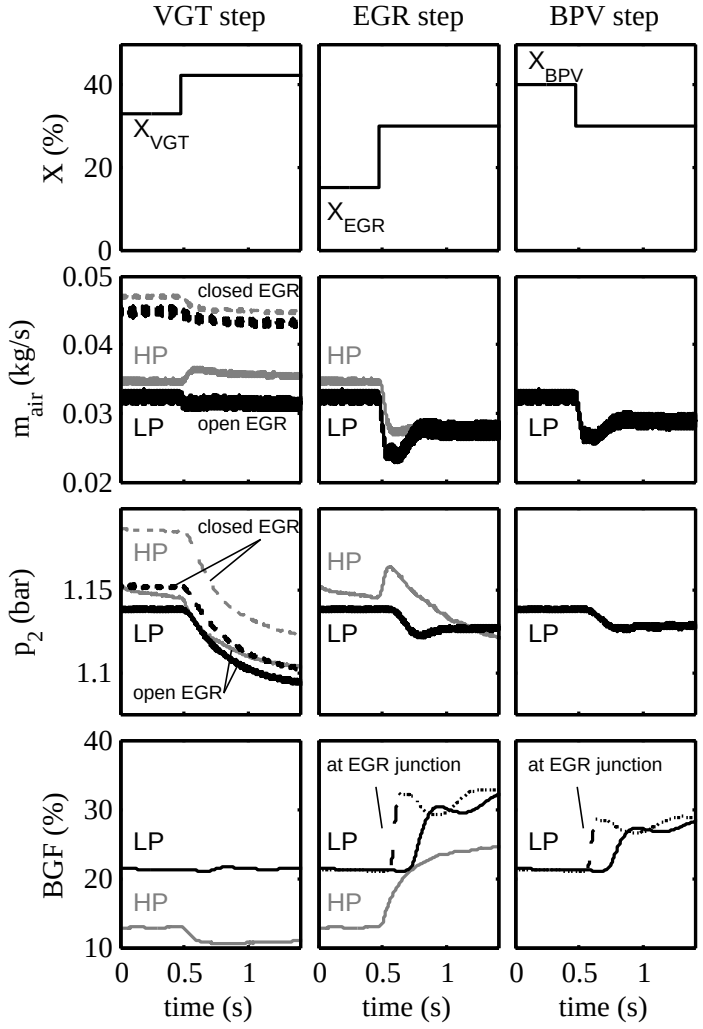

Figure 10: Results of the HP-EGR system (—) and the LP-EGR system (—) for steps in the different control variables at 2400 rpm and 20 mg/str (conditions D). Left: step in VGT position, for partially open EGR (full) and closed EGR (broken). Centre: step in EGR position (dashed: BGF downstream the EGR junction). Right: step in BPV position (dashed: BGF downstream the EGR junction).

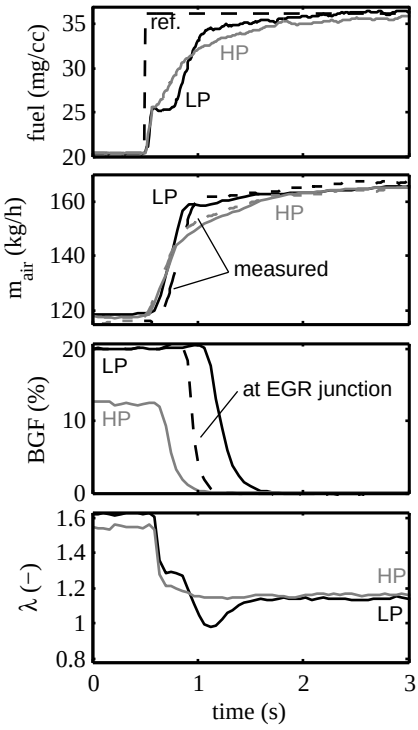

Figure 11: Evolution during a load response for the HP-EGR configuration (—) and the LP-EGR configuration (—). Dotted lines in the m_a plot correspond to experimental values; BGF and λ were obtained after fitting OpenWAM model to the experimental test.

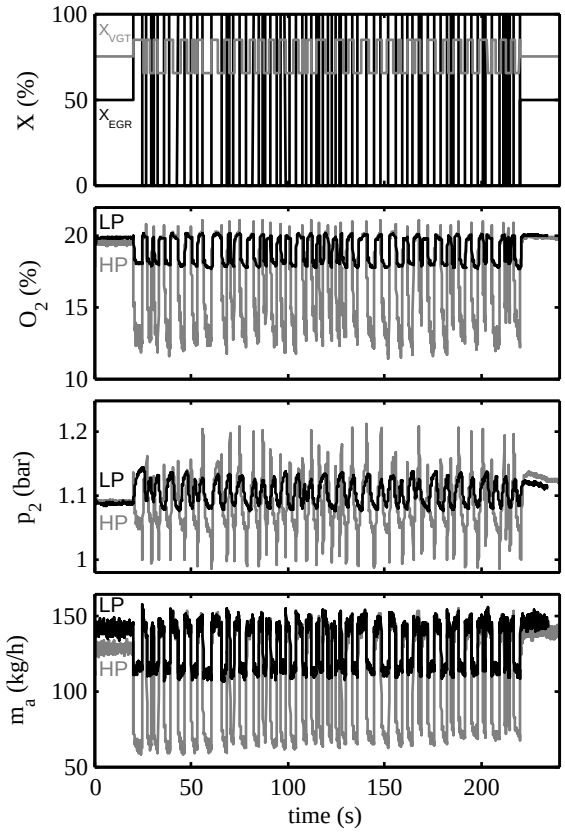

Figure 12: Evolution of O_2, p_2 and m_a for a pseudo-random binary sequence in VGT and EGR positions with HP-EGR architecture (—) compared with LP-EGR layout (—) at 2400 rpm and 20 mg/str (conditions D).

HP-EGR architecture.

From results presented in Figure 12 it can be concluded that LP-EGR presents a quasi-linear behaviour, while this is not the case of the HP-EGR system due to the sign inversions and non-minimum phase behaviours that were discussed previously. In fact, the only nonlinear effect that exists in the LP-EGR configuration is associated with the variation of the output gain for different actuator positions. This may be corrected through a Hammerstein model, which combines a nonlinear static correction of the control action with dynamic linear model [34]. With the proper correction of the nonlinear system gain, the identified model provides an almost perfect prediction of the LP-EGR system behaviour. This is illustrated the in right-hand plots of figure 13, where the results of the model are compared to the measured signal for the first 50 seconds of the test shown in Figure 12.

On the other hand, if the same modelling approach is used for the HP-EGR configuration, the model is not able to provide a correct prediction of the system, as it is shown in left-hand plots of figure 13. Significantly in the case of boost pressure the existence of the non-minimum phase behaviour with the EGR opening becomes evident [35]. The existence of such effects in

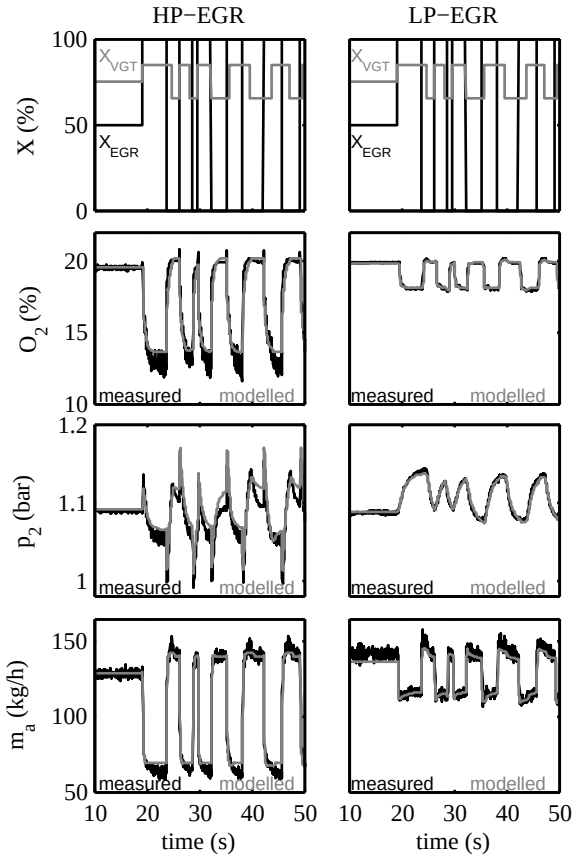

Figure 13: Hammerstein model identified (—) compared with wave action model results (—) at 2400 rpm and 20 mg/str (conditions D). Left: HP-EGR; right: LP-EGR.

the HP-EGR system, along with sign reversals and saturations in the actuators authority [36], significantly complicate its control. In order to deal with it, some authors have proposed using non-linear compensators [29], or a model-based approach that shifts between different controllers according to the EGR valve position, engine speed and load [30]; however, in many industrial applications, air mass flow and boost pressure are not closed-loop controlled at the same time, in order to improve system robustness [37]. The results obtained when modelling the LP-EGR, and the almost decoupled behaviour of the EGR and VGT, suggest that easier control solutions may be used.

7. Conclusions

The present paper shows a comparison between HP- and LP-EGR architectures from the point of view of engine control. A set of experimental and modelling studies have been carried out to reach the following conclusions:

- The long path followed by the gas from the air-EGR junction to the cylinders allows a perfect mixing between this two species; then a broadband lambda sensor placed anywhere in the intake manifold provides a representative value of the intake O_2 concentration. On the contrary, the non homogeneity in the intake charge when HP-EGR configurations are used prevents lambda sensor measurement from being representative of the real cylinder intake O_2 concentration, which involves difficulties when this sort of sensors are used with control purposes.

- The static gain analysis has shown that with the LP-EGR system the BGF is decoupled from the VGT opening; similarly, the intake pressure is almost independent of the EGR valve opening. On the contrary, a strong coupling between the previous signals is observed with the HP-EGR architecture. Regarding the air mass flow, a gain inversion has been observed with the HP-EGR loop, since the VGT closing leads to an air mass flow increase when the EGR valve is closed, but an air mass flow decrease when the EGR valve is large open. This behaviour has not been observed with the LP-EGR architecture.

- From the static gain analysis, a study of the signal pairing for air management control has been carried out. The main conclusion is that the coupling between EGR and VGT with the HP-EGR layout make air path control tasks difficult: when the standard control pair $\{m_a, p_2\}$ is chosen there is a risk of instability when the VGT is closed and a simultaneous control of both variables is required; if the control pair $\{p_2, BGF\}$ is selected, the system will be stable, but strongly coupled. On the contrary, with the LP-EGR architectures the air path can be more easily controlled with both $\{m_a, p_2\}$ and $\{p_2, BGF\}$. Particularly, the control set $\{p_2, BGF\}$ is specially suitable for the LP-EGR loop since the BGF does not depend on the VGT opening, and the EGR valve hardly affects intake pressure. As far as the control pair $\{m_a, BGF\}$ is concerned, the engine behaviour with this control set is unstable regardless the EGR loop employed due to the strong effect of the EGR opening on both control variables.

- The dynamic analysis has confirmed the conclusions obtained from the static maps presented, and also has shown the non-minimum phase behaviour of the p_2 with the EGR opening when the HP-EGR configuration is used. In addition, from the dynamic analysis the important BGF delay with the LP-EGR loop can be observed. This delay is due to the high distance between the air-EGR junction and the cylinders.

- The experiment with pseudo-random binary evolutions for both EGR and VGT positions has allowed to conclude that while the LP-EGR loop shows a quasi-linear behaviour, the HP-EGR architecture involves important non-linearities that restrict the linear identification to local regions.

Some of the reported effects significantly depend on the operating conditions for the tested engine; however identified features are expected to appear in other diesel engines. In the case of the concentration non-homogeneity for the HP-EGR architecture, the geometric design of the EGR feed and of the intake manifold will be a key factor. On the other hand, sign inversions and other non-linearities in HP-EGR loop will appear depending on the selected engine, the operating range and the effective range of the actuators.

Acknowledgement

This research has been partially financed by the Spanish Ministerio de Economía y Competitividad, thorugh project IPT-370000-2010-022 "Investigación y desarrollo de tecnologías de EGR adaptadas a las nuevas arquitecturas y requerimientos de refrigeración en motores diesel sobrealimentados para automoción (HIREFIRE)".

References

[1] N. Ladommatos, S. Abdelhalim, H. Zhao, The effects of exhaust gas recirculation on diesel combustion and emissions, International Journal of Engine Research 1 (1999) 107–126.

[2] M. Lapuerta, J. Hernández, F. Gimenez, Evaluation of exhaust gas recirculation as a technique for reducind diesel engine NOx emissions, Proc. Inst. Mech. Eng. Part D-J. Automob. Eng. 214 (2000) 85–93.

[3] R. Baert, D. Beckman, A. Veen, Efficient EGR technology for future HD diesel engine emission targets, SAE paper 1999-01-0837.

[4] S. Moroz, G. Bourgoin, J. Luján, B. Pla, A 2.0 litre diesel engine with low pressure exhaust gas recirculation and advanced cooling system, The Diesel Engine Conference, Proceedings of the SIA 2008 Conference, Rouen, France.

[5] A. Walker, Controlling particulate emissions from diesel vehicles, Topics in Catalysis 28 (2004) 165–170.

[6] S. Krüger, UandEdwards, E. Pantow, R. Lutz, R. Dreisbach, M. Glensvig, High performance cooling and EGR systems as a contribution to meeting future emission standards, SAE paper 2008-01-1199.

[7] M. Jankovic, M. Jankovic, I. Kolmanovsky, Constructive Lyapunov control design for turbocharged diesel engines, IEEE Transactions on Control System Technology 8(2) (2000) 288–299.

[8] I. Kolmanovsky, A. Stefanopoulou, P. Moraal, M. van Nieuwstadt, Issues in modeling and control of intake flow in variable geometry turbocharged engines, Proceedings of the 18th IFIP COnference on System Modeling and Optimization, Detroit July 1997.

[9] J. Rückert, Schloß, H. Rake, B. Kinoo, M. Krüger, S. Pischinger, Model based boost pressure and exhaust gas recirculation rate control for a diesel engine with variable turbine geometry, IFAC Workshop: Advances in Automotive Control.

[10] M. Ammann, N. Fekete, L. Guzella, A. Glattfelder, Model-based control of the VGT and EGR in a turbocharged common-rail diesel engine: Theory and passenger car implementation, SAE paper 2003-01-0357.

[11] J. Merten, K. Glover, U. Christen, Comparison of uncertainty parametrisations for h_∞ robust control of turbocharged diesel engines, Control engineering practice.

[12] R. Ramajani, Control of a variable-geometry turbocharged and wastegated diesel engine, Proceedings of the Institution of Mechanical Engineers, Part D: Journal of Automobile Engineering 219 (2005) 1361–1368.

[13] P. Ortner, L. del Re, Predictive control of a diesel engine air path, IEEE Transactions on Control Systems Technology 15(3) (2007) 449–456.

[14] M. van Nieuwstadt, I. Kolmanovsky, P. Moraal, A. Stefanopoulou, M. Jankovic, EGR-VGT control schemes: Experimental comparison for a high-speed diesel engine, IEEE Control Systems Magazine 20 (2000) 63–79.

[15] A. Stefanopoulou, I. Kolmanovsky, J. Freudenberg, Control of variable geometry turbocharged diesel engines for reduced emissions, IEEE Transactions on Control Systems Technology 8 (2000) 733–745.

[16] B. Youssef, G. Le Solliec, G. Corde, O. Hayat, C. Jabeur, P. Calendini, Low pressure EGR control for a turbocharged diesel HCCI engine, 18th IEEE International Conference on Control Applications. Part of 2009 IEEE Multi-conference on Systems and Control (2009) 346–351.
[17] J. Galindo, H. Climent, C. Guardiola, J. Doménech, Modeling the vacuum circuit of a pneumatic valve system, Journal of Dynamic Systems, Measurement and Control, Transactions of the ASME 131 (3) (2009) 1–11.
[18] J. Galindo, J. Serrano, F. Arnau, P. Piqueras, Description and analysis of a one-dimensional gas-dynamic model with independent time discretization, Proceedings of the ASME Internal Combustion Engine Division 2008 Spring Technical Conference.
[19] J. Galindo, F. J. Arnau, A. Tiseira, P. Piqueras, Solution of the turbocompressor boundary condition for one-dimensional gas-dynamic codes, Mathematical and Computer Modelling 52 (7-8) (2010) 1288–1297.
[20] J. Serrano, H. Climent, C. Guardiola, P. Piqueras, Methodology for characterisation and simulation of turbocharged diesel engines combustion during transient operation. Part 2: Phenomenological combustion simulation, Applied Thermal Engineering 29 (2009) 150–158.
[21] J. Galindo, H. Climent, C. Guardiola, A. Tiseira, J. Portalier, Assessment of a sequentially turbocharged diesel engine on real-life driving cycles, International Journal of Vehicle Design 49 (1-3) (2009) 214–234.
[22] J. Serrano, H. Climent, C. Guardiola, P. Piqueras, Methodology for characterisation and simulation of turbocharged diesel engines combustion during transient operation. part 2: Phenomenological combustion simulation, Applied Thermal Engineering 29 (1) (2009) 150–158.
[23] V. Macián, J. Galindo, J. Luján, C. Guardiola, Detection and correction of injection failures in diesel engines on the basis of turbocharger instantaneous speed frequency analysis, Proceedings of the Institution of Mechanical Engineers, Part D: Journal of Automobile Engineering 219 (5) (2005) 691–701.
[24] J. Luján, J. Galindo, J. Serrano, B. Pla, A methodology to identify the intake charge cylinder-to-cylinder distribution in turbocharged direct injection diesel engines, Measurement Science and Technology 19 (6) (2008) 065401.
[25] C. Guardiola, A. Gil, B. Pla, P. Piqueras, Representation limits of mean value engine models, Lecture Notes in Control and Information Sciences 418 (2012) 185–206.
[26] A. Amstutz, L. del Re, EGO sensor based robust output control of EGR in diesel engines, IEEE Transactions on Control Systems Technology 3(1) (1995) 37–48.
[27] J. Arrègle, J. López, C. Guardiola, C. Monin, Sensitivity study of a NOx estimation model for on-board applications, SAE paper 2008-01-0640.
[28] L. Guzzella, A. Amstutz, Control of diesel engines, IEEE Control Systems 18(5) (1998) 53–71.
[29] J. Wahlström, L. Eriksson, L. Nielsen, EGR-VGT control and tuning for pumping work minimization and emission control, IEEE Transactions on Control Systems Technology 18(4) (2010) 993–1003.
[30] P. Langthaler, L. Del Re, Fast predictive oxygen charge control of a diesel engine, Proceedings of the American Control Conference (2007) 4388–4393.
[31] C.-J. Chiang, A. Stefanopoulou, M. Jankovic, Nonlinear observer-based control of load transitions in homogeneous charge compression ignition engines, IEEE Trans. on Cont. Sist. Technol. 15 (2007) 438448.
[32] C. Beatrice, G. Avolio, C. Bertoli, N. Del Giacomo, C. Guido, M. Migliaccio, Critical aspects on the control in the low temperature combustion systems for high performance di diesel engines, Oil Gas Sci. Technol. 62 (2007) 471–482.
[33] E. Bristol, New measure of interaction for multivariable process control, IEEE Transactions on Automatic Control 11 (1965) 133–134.
[34] F. Giri, F. Chaoui, Y. Rochdi, Parameter identification of a class of hammerstein plants, Automatica 37 (5) (2001) 749 – 756.
[35] J. Wahlström, L. Eriksson, Performance gains with egr-flow inversion for handling non-linear dynamic effects in egr vgt ci engi..., Fifth IFAC Symposium on Advances in Automotive Control,2007 s. 531-538.
[36] A. Stefanopoulou, I. Kolmanovsky, J. Freudenberg, Control of variable geometry turbocharged diesel engines for reduced emissions, Control Systems Technology, IEEE Transactions on 8 (4) (2000) 733 –745.
[37] F. Payri, J. Lujàn, C. Guardiola, G. Lapuente, Experimental evaluation of the impact of vgt control malfunction on pollutant emissions, Proceedings of the ECOSM New Trands in Engine COntrol, Simulation and Modelling.